Regenerative Therapy 21 (2022) 239–249

Contents lists available at ScienceDirect

Regenerative Therapy

journal homepage: http://www.elsevier.com/locate/reth

Original Article

SHOX2 refines the identification of human sinoatrial nodal cell population in the in vitro cardiac differentiation

Takayuki Wakimizu [a], Kumi Morikawa [a, b, 1], Kenta Fukumura [a, 2], Tetsuo Yuki [a], Takashi Adachi [a, 3], Yasutaka Kurata [c], Junichiro Miake [d], Ichiro Hisatome [a], Motokazu Tsuneto [a, *], Yasuaki Shirayoshi [a]

[a] *Division of Regenerative Medicine and Therapeutics, Department of Genetic Medicine and Regenerative Therapeutics, Tottori University Graduate School of Medical Science, 86 Nishi-cho, Yonago, Tottori 683-8503, Japan*
[b] *Center for Promoting Next-Generation Highly Advanced Medicine, Tottori University Hospital, 36-1 Nishi-cho, Yonago, Tottori 683-8504, Japan*
[c] *Department of Physiology II, Kanazawa Medical University, 1-1 Daigaku, Uchinada- Machi, Kahoku-gun, Ishikawa 920-0293, Japan*
[d] *Department of Pharmacology, Tottori University Graduate School of Medical Science, 86 Nishi-cho, Yonago, Tottori 683-8503, Japan*

ARTICLE INFO

Article history:
Received 15 February 2022
Received in revised form
22 June 2022
Accepted 23 July 2022

Keywords:
SHOX2
HCN4
hiPSCs
Sinoatrial node

ABSTRACT

Introduction: Dysfunction of the sinoatrial node (SAN) cells causes arrhythmias, and many patients require artificial cardiac pacemaker implantation. However, the mechanism of impaired SAN automaticity remains unknown, and the generation of human SAN cells in vitro may provide a platform for understanding the pathogenesis of SAN dysfunction. The short stature homeobox 2 (*SHOX2*) and hyperpolarization-activated cyclic nucleotide-gated cation channel 4 (*HCN4*) genes are specifically expressed in SAN cells and are important for SAN development and automaticity. In this study, we aimed to purify and characterize human SAN-like cells in vitro, using *HCN4* and *SHOX2* as SAN markers.
Methods: We developed an HCN4-EGFP/SHOX2-mCherry dual reporter cell line derived from human induced pluripotent stem cells (hiPSCs), and *HCN4* and *SHOX2* gene expressions were visualized using the fluorescent proteins EGFP and mCherry, respectively. The dual reporter cell line was established using an HCN4-EGFP bacterial artificial chromosome-based semi-knock-in system and a CRISPR-Cas9-dependent knock-in system with a SHOX2-mCherry targeting vector. Flow cytometry, RT-PCR, and whole-cell patch-clamp analyses were performed to identify SAN-like cells.
Results: Flow cytometry analysis and cell sorting isolated HCN4-EGFP single-positive ($HCN4^+/SHOX2^-$) and HCN4-EGFP/SHOX2-mCherry double-positive ($HCN4^+/SHOX2^+$) cells. RT-PCR analyses showed that SAN-related genes were enriched within the $HCN4^+/SHOX2^+$ cells. Further, electrophysiological analyses showed that approximately 70% of the $HCN4^+/SHOX2^+$ cells exhibited SAN-like electrophysiological characteristics, as defined by the action potential parameters of the maximum upstroke velocity and action potential duration.
Conclusions: The HCN4-EGFP/SHOX2-mCherry dual reporter hiPSC system developed in this study enabled the enrichment of SAN-like cells within a mixed $HCN4^+/SHOX2^+$ population of differentiating cardiac cells. This novel cell line is useful for the further enrichment of human SAN-like cells. It may contribute to regenerative medicine, for example, biological pacemakers, as well as testing for cardiotoxic and chronotropic actions of novel drug candidates.

* Corresponding author. 86 Nishi-cho, Yonago, Tottori 683-8503, Japan.
E-mail address: mtsuneto@tottori-u.ac.jp (M. Tsuneto).
Peer review under responsibility of the Japanese Society for Regenerative Medicine.
[1] Present address: Department of Life Science and Biotechnology, Health and Medical Research Institute, National Institute of Advanced Industrial Science and Technology (AIST), Central 6, 1-1-1 Higashi, Tsukuba, Ibaraki 305–8566, Japan.
[2] Present address: Biochemistry Team, Bio Science Division, Technology General Division Material Integration Laboratories, AGC Inc., 1-1 Suehiro-cho, Tsurumi-ku, Yokohama, Kanagawa 230–0045, Japan.
[3] Present address: Minaris Regenerative Medicine Co. Ltd., Shibusawa Building, 1, Ebisu-cho, Kanagawa-ku, Yokohama-shi, Kanagawa 221–0024, Japan.

https://doi.org/10.1016/j.reth.2022.07.012

List of abbreviations

ACT-B	actin beta
AP	action potential
APA	AP amplitude
APD	AP duration
BAC	bacterial artificial chromosome
BMP4	bone morphogenetic protein 4
BPM	beats per minute
CCS	cardiac conduction system
CL	cycle length
CM	cardiomyocyte
DMEM	Dulbecco's modified Eagle's medium
dV/dt_max	maximal rate of depolarization
FBS	fetal bovine serum
FHF	first heart field
FACS	fluorescent-activated cell sorting
Gi	GSK3 inhibitor
HA	homology arm
HCN4	hyperpolarization-activated cation channels 4
hESC	human embryonic stem cell
hPSC	human pluripotent stem cell
hiPSC	human induced pluripotent stem cell
KSR	knock-out serum replacement
MDP	maximum diastolic potential
MEF-CM	MEF-conditioned medium
MEF	mouse embryonic fibroblast
MYL2	myosin light chain 2
NEAA	nonessential amino acid
NR2F2	nuclear receptor subfamily 2 group F member 2
SAN	sinoatrial node
SHF	second heart field
SHOX2	short stature homeobox 2
TBX	T-box transcription factor
TNNT2	troponin T2
Wi	WNT inhibitor
2-ME	2-mercaptoethanol

1. Introduction

Sinoatrial node (SAN) cells function as pacemakers in the heart via their inherited electrical automaticity. Dysfunction of SAN cells causes sick sinus syndrome (SSS), in which the patient suffers from bradycardias and requires the implantation of pacemaker devices [1]. However, studies on the physiology of human SAN cells and the pathophysiology of SSS have been hampered by the difficulty of obtaining human SAN cells.

Human induced pluripotent stem cells (iPSCs) give rise to cardiomyocytes (CMs) in vitro, which has made it possible to study the physiology and pathology of human CMs [2–4]. Human iPSC-derived CMs are heterogeneous cell populations comprising myocytes of the cardiac conduction system as well as those of cardiac chambers, atrium, and ventriculus [5]. To identify specific cell populations in iPSC-derived CMs, specific differentiation systems, cell surface markers, or reporter genes have been employed. To identify SAN-like cells based on the expression of pacemaker genes and observation of spontaneous electrical automaticity, CD166-positive cell populations, TBX3-positive cell populations, NKX2.5-negative, CD90-negative, and SIRPA-positive cell populations, and hyperpolarization-activated cyclic nucleotide-gated cation channel 4 (HCN4)-positive cell populations have been identified as SAN-like cell populations [6–10]. However, in recent years, in vitro iPSC-derived CMs have expressed pacemaker genes such as the HCN family at an early stage, with spontaneous electrical automaticity showing a heterogeneous population [11]. Previous evaluation of gene labeling and automaticity alone may have been inadequate in electrophysiologically labeling iPSC-derived SAN-like cells with the characteristics of native SAN cells. Moreover, SAN-like cells have shown distinct characteristics of spontaneous action potentials from those of atrial and ventricular-like cells, although it is still unclear how to identify SAN-like cell populations with SAN-like spontaneous action potentials.

We hypothesized that the use of short stature homeobox 2 (SHOX2), a SAN-specific transcription factor gene [12], together with HCN4 may improve the identification of SAN-like cells with spontaneous action potentials close to those of native cardiac pacemaker cells. To test this hypothesis, we created human iPSCs using dual reporters of SHOX2 and HCN4. We found an $HCN4^+/SHOX2^-$ and $HCN4^+/SHOX2^+$ cell population but not in the $SHOX2^+/HCN4^-$ cell population. Molecular, electrophysiological, and pharmacological tests revealed that the $HCN4^+/SHOX2^+$ cell population comprised more SAN-like cells than the $HCN4^+/SHOX2^-$ cell population. We conclude that SHOX2 refines the identification of human SAN-like cell populations during in vitro cardiac differentiation.

2. Materials and methods

2.1. Cell culture and establishment of the HCN4/SHOX2 dual reporter hiPSC line

hiPSCs were maintained on mitomycin-C-treated mouse embryonic fibroblasts (MEFs) in hiPSC medium comprising the following: Dulbecco's modified Eagle's medium (DMEM)/F12 (Sigma–Aldrich, St. Louis, MO, USA); 20% knock-out serum replacement (KSR, Thermo Fisher Scientific, Waltham, MA, USA); 1x GlutaMAX (Gibco; Thermo Fisher Scientific); 1x nonessential amino acids (NEAAs, Sigma); 0.1 mM 2-mercaptoethanol (2-ME, Sigma); 5 ng/ml recombinant human FGF2 (Wako, Osaka, Japan). The cells were passaged every four days by enzymatic dissociation using a CTK solution comprising 1 mg/ml collagenase type IV (Gibco), 0.25% trypsin without phenol red (Gibco), 20% KSR, and 1 mM $CaCl_2$ (Wako) in D-PBS (Wako).

The HCN4-EGFP/SHOX2-mCherry dual reporter hiPSC line was established by transgenesis of an HCN4-EGFP BAC-based semi-knock-in vector, followed by CRISPR/cas9-mediated genome editing with a SHOX2-mCherry targeting vector in the wild-type 409B2 hiPSC line [13]. First, we constructed an HCN4-EGFP targeting vector, which had HCN4 homology arms (HAs) cloned from 409B2 cells, EGFP, and FRT-PGK-neo-FRT selection cassettes (Supplementary Fig. 1A). The left and right HCN4 HAs were designed to be upstream and downstream of the HCN4 ATG start codon in exon I. Using the HCN4-EGFP targeting vector, the HCN4-EGFP-BAC transgene was generated by homologous recombination at the HCN4 locus in an RP11-1105A6 BAC vector using a Red-ET system (Gene Bridge, USA). After the transfection of the HCN4-EGFP-BAC transgene into 409B2 cells and drug selection, the hiPSC line harboring the intact HCN4-EGFP-BAC

transgene was confirmed by PCR. HCN4-EGFP single reporter hiPSCs were finally established through treatment with pCAG-Flpo (Gene Bridge, USA), which removed the PGK-neo selection cassette.

Next, HCN4-EGFP/SHOX2-mCherry dual reporter hiPSCs were established by transfection of a *SHOX2* targeting vector with mCherry into HCN4-EGFP hiPSCs. The SHOX2-mCherry targeting vector carried the *SHOX2* HAs, mCherry, and VloxP-PGK-neo-VloxP sequences (Supplementary Fig. 1B). *SHOX2* HAs were cloned from HCN4-EGFP hiPSCs, and the left and right HAs were designed upstream and downstream of the *SHOX2* ATG start codon. Following transfection of the *SHOX2* vector and drug selection, we confirmed the SHOX2-mCherry locus by performing genomic PCR and generated the HCN4-EGFP BAC transgenic/SHOX2-mCherry knock-in dual reporter hiPSC line (HCN4-EGFP/SHOX2-mCherry hiPSC line).

For plasmid DNA transfection by electroporation, 1×10^6 HCN4-EGFP single reporter hiPSCs isolated by TrypLE Select (Thermo Fisher Scientific) were suspended at a density of 1×10^7 cells/ml in resuspension buffer R (Thermo Fisher Scientific) containing 25 μg of a linearized targeting vector and 5 μg of a CRISPR-Cas9 vector with guide RNA. Electroporation was performed using a Neon transfection system (Thermo Fisher Scientific) with the following parameters: 1100 V, 30 ms (pulse width), and 1 pulse. The cells were seeded with neomycin-resistant MEFs and 10 μM Y-27632, a Rho-associated coiled-coil-containing protein kinase inhibitor. Antibiotic selection was initiated with 50 μg/ml G418 (Thermo Fisher Scientific) three days after transfection. To confirm that the targeting vector was knocked into the target gene locus, half of the selected colonies were subjected to direct PCR screening. The other half of the colony was expanded for further analysis following PCR confirmation of a successful target locus knock-in.

2.2. Cardiac cell differentiation

For cardiac differentiation of hiPSCs, we used two protocols named “Gi protocol” (Supplementary Fig. 2A) and “GiWi protocol” (Fig. 1A) [14,15].

To establish a feeder-free culture, small clumps of cells were transferred into Corning® Matrigel® matrix (with a reduced concentration of growth factor; Corning, NY, USA)-coated dishes and cultured with MEF-conditioned medium (MEF-CM) for 24 h. The next day, referred to as day 0 of culture, cells were cultured in N2B27 medium comprising the following: DMEM/F12 supplemented with 1% N2 (Gibco); 2% B27 (Gibco); glycogen synthase kinase 3 (GSK3) inhibitor CHIR99021 at 3.3 μM (Axon Medchem BV, Groningen, Netherlands); 200 ng/ml recombinant human Noggin/Fc chimera (R&D Systems, Minneapolis, MN, USA) for 72 h. On day 3, the cells were cultured in the N2B27 medium supplemented with the Wnt inhibitor IWP-2 at 5 μM (Cayman Chemical, Ann Arbor, MI, USA) and 200 ng/ml recombinant human Noggin/Fc chimera for 24 h (“GiWi protocol”). On day 3 (on day 4 at “GiWi protocol”) of the culture, the cells were trypsinized, seeded at a density of 1×10^6 cells per well in 6-well ultralow attachment plates (Corning). Subsequently, they were cultured in RPMI 1640 medium (Thermo Fisher Scientific) supplemented with the following: 0.5% fetal bovine serum (FBS); 2 mM L-ascorbic acid; 10 mM nicotinamide; 0.2 μM dexamethasone; 1% insulin-transferrin-selenium (Thermo Fisher Scientific); 1% sodium pyruvate solution (WAKO); 10 ng/ml recombinant human bone morphogenetic protein 4 (BMP4) (R&D Systems). After culturing in BMP4-containing medium for 14 days, BMP4 was removed from the medium, and BMP4-free medium was refreshed every 4–7 days.

2.3. Flow cytometry analysis and cell sorting

Aggregates cultured were dissociated by incubating for 20 min with activated papain (Worthington, Columbus, OH, USA) at 37 °C. Cells from the small clumps that remained after papain dissociation were incubated for 10 min with 40 mg/ml collagenase type II (Worthington) at 37 °C. Single-dissociated cells were washed with PBS containing 2% FBS. Flow cytometry was performed using a BD LSRFortessa flow cytometer (Becton, Dickinson and Company, Franklin Lakes, NJ, USA). Further, cell sorting was performed using a MoFlo XDP (Beckman Coulter, Brea, CA, USA). Moreover, 4′,6-Diamidino-2-phenylindole (DAPI, Wako) was used to eliminate dead cells, and 409B2 cells were used as control hiPSCs [13] to set the control gates for FACS.

2.4. RNA extraction, cDNA synthesis, and time PCR analysis

Total RNA was isolated using an RNeasy Micro Kit (Qiagen). cDNA was synthesized using a PrimeScript® RT reagent kit with gDNA Eraser (Perfect Real Time; TaKaRa Bio, Kusatsu, Japan). RT-PCR was performed using EmeraldAmp® MAXPCR Master Mix (TaKaRa Bio). Primer sequences are listed in Supplementary Table 1.

2.5. Electrophysiology

For measurements of the action potential (AP) and membrane currents by the whole-cell patch-clamp method, sorted HCN4-EGFP/SHOX2-mCherry dual reporter hiPSC-derived CMs (3×10^3 cells/30 μl drop) were cultured on Matrigel-coated glass coverslips for 3 days at 37 °C. APs and HCN4-mediated hyperpolarization-activated cation channel currents (I_f) in CMs were measured by the perforated patch-clamp technique using 250 μg/ml amphotericin B (Sigma) with an Axopatch-200 B amplifier (Molecular Devices, San Jose, CA, USA). I_f currents were evoked by 1.5-s test pulses ranging from −60 to −150 mV in 10 mV decrements with a holding potential of −60 mV in the voltage-clamp mode. Generation of the voltage pulses, data acquisition, and data analyses were performed using pCLAMP 9 software (Molecular Devices). Cells were perfused with normal Tyrode's solution with the following composition: 140 mM NaCl, 5.4 mM KCl, 1.8 mM $CaCl_2$, 0.5 mM $MgCl_2$, 0.33 mM $NaHPO_4$, 5 mM HEPES, and 5 mM glucose (pH 7.4 adjusted with NaOH). The internal pipette solution contained 130 mM K-glutamate, 1 mM $MgCl_2$, 15 mM KCl, 5 mM NaOH, 5 mM HEPES, and 5 mM Mg-ATP (pH 7.3, adjusted with potassium hydroxide). Each recording pipette had a tip resistance of approximately 7–8 MΩ when filled with the internal solution containing amphotericin B. All measurements were performed at 37 ± 2 °C. Cell membrane capacitances were 21.8 ± 1.7 pF.

2.6. Statistical analysis

All data are presented as mean ± SD or SEM. Statistical significance was determined in R (v4.1.1) using the Fisher's test and the Mann–Whitney U test for two-group comparisons.

2.7. Internal staining of TNNT2

Aggregates cultured for 60 days were dissociated by incubating for 12 h with 40 mg/ml collagenase type II (Worthington, Columbus, OH, USA) at 25 °C. Cells were passed through a 70 μm filter and fixed with 4% PFA (Nacalai tesque, Tokyo, Japan) for 10 min at 25 °C. After permeabilization of cells with permeabilization buffer (BioLegend Japan, Tokyo, Japan), cells were stained with Alexa Fluor®647 (Alexa 647) mouse anti-cardiac troponin T antibody (Becton, Dickinson and Company). Flow cytometry was performed

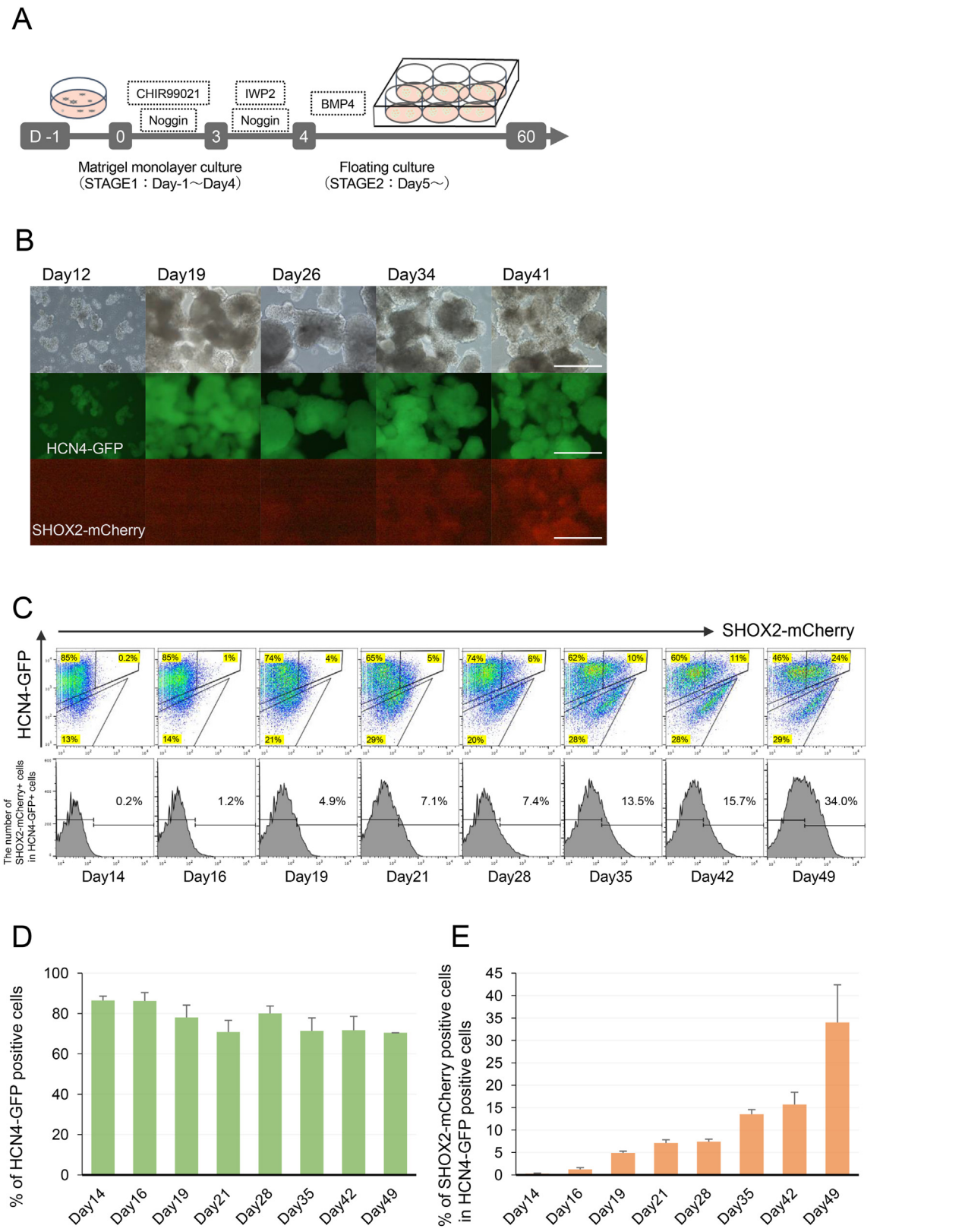

Fig. 1. . Differentiation of the HCN4-EGFP BAC transgenic and SHOX2-mCherry knock-in human induced pluripotent stem cell (hiPSC) into cardiomyocytes (CMs) in vitro using the GSK3 inhibitor (Gi) CHIR99021 and WNT inhibitor (Wi) IWP2 (GiWi protocol). (A) A scheme of the GiWi protocol. (B) Representative images of cardiac aggregates expressing EGFP and mCherry recorded on culture days 12, 19, 26, 34, and 41. Scale bars indicate 500 μm. (C) Flow cytometry analysis of cardiac differentiation of dual reporter hiPSCs on days 14–49. (D) Percentages of HCN4-EGFP-positive cells during cardiac differentiation as analyzed by flow cytometry shown in Panel C (n=4). (E) Percentages of the HCN4-EGFP/SHOX2-mCherry double-positive cells in the HCN4-EGFP-positive cell population during differentiation as shown in Panel C (n=4).

using a BD LSRFortessa flow cytometer (Becton, Dickinson and Company).

2.8. Computer simulation of spontaneous action potentials

To show the effect of I_f block on spontaneous action potentials of human SAN cells, we performed computer simulations using a mathematical model describing electrical behaviors of human SAN cells developed by Fabbri et al. [39]. Dynamic behaviors of the model cell were determined by solving a system of non-linear ordinary differential equations numerically. Numerical computations were performed with MATLAB 7.5 (The MathWorks, Natick, MA, USA) on Workstation HP Z800 (Hewlett–Packard, Tokyo, Japan). We used a variable time-step numerical differentiation approach selected for its suitability for stiff systems, which is available as an ordinary differential equation solver, *ode15s*, in MATLAB. Detailed model structures (a complete list of the equations and standard parameter values for the model cell) and simulation procedures are described in the previous articles [39–41].

3. Results

3.1. HCN4/SHOX2 dual reporter system identifies subpopulations in HCN4 cell populations

We differentiated HCN4-EGFP/SHOX2-mCherry hiPSCs into CMs using two CM induction protocols: the Gi protocol using GSK3 inhibitor CHIR99021 (also called "Yamauchi protocol") and the GiWi protocol using CHIR99021 and the Wnt inhibitor IWP-2. These methods comprise two steps. For the Gi protocol, the mesodermal population was induced by inhibiting GSK3 signaling for 3 days (Stage 1). Subsequently, hiPSCs were differentiated into CMs in suspension culture with BMP4 (Stage 2) (Supplementary Fig. 2A). For the GiWi protocol, the mesodermal population was generated by inhibiting the GSK3 signal for the first 3 days, followed by inhibiting the Wnt signal for 1 day (Stage 1), and differentiation into CMs in suspension culture with BMP4 (Stage 2) (Fig. 1A). Microscopic analysis performed after both protocols indicated that HCN4-EGFP- and SHOX2-mCherry-expressing cells were detected after 12 and 34 days of culture, respectively (Fig. 1B). All HCN4-EGFP-expressing cells began beating on day 12. In addition, we checked the consistency of endogenous mRNA expression and the reporter protein expression with the GiWi protocol. RT-PCR results showed that *HCN4* and GFP, *SHOX2*, and mCherry mRNA expression, were correlated with each other. *HCN4* and GFP were expressed from day 14 to day 42 constantly; *SHOX2* and mCherry were a little expressed on day 14 and the expression was increased gradually until day 42 (Supplementary Fig. 3). In HCN4-GFP/SHOX2-mCherry hiPSC line, each reporter protein expression was reflecting the endogenous mRNA expression (Fig. 1).

Flow cytometric analysis revealed both HCN4-EGFP single-positive cells ($HCN4^+/SHOX2^-$) and HCN4-EGFP/SHOX2-mCherry double-positive cells ($HCN4^+/SHOX2^+$), although the $SHOX2^+/HCN4^-$ cell population was not observed (Fig. 1C, Supplementary Fig. 2B). Using the Gi protocol, the percentage of HCN4 expressing cells increased to 58% of the total cell population on day 14 and gradually decreased to 10% (Supplementary Fig. 2C). Conversely, with the GiWi protocol, HCN4 expressing cells increased to 85% of the total cell population on day 14 and then decreased to approximately 70% (Fig. 1D). With both protocols, $HCN4^+/SHOX2^+$ appeared in the $HCN4^+/SHOX2^-$ population on day 16 of culture, and $HCN4^+/SHOX2^+$ in the HCN4 expressing cell population increased to 34% (GiWi protocol) and 44% (Gi protocol) by day 49 (Fig. 1E, Supplementary Fig. 2D).

3.2. $HCN4^+/SHOX2^+$ cell population represent biochemical properties of SAN-like cells

To check if the $HCN4^+$ cell population contained cardiomyocytes, we analyze the *TNNT2* protein expression. Intracellular immunostaining-based FACS showed that 69.6% of $HCN4^+/SHOX2^-$ cells expressed TNNT2 and 88.8% of $HCN4^+/SHOX2^+$ cells expressed TNNT2 (Supplementary Fig. 4A). To characterize each population, we isolated $HCN4^+/SHOX2^-$ and $HCN4^+/SHOX2^+$ cells by cell sorting on day 60 and examined their mRNA expression (Fig. 2). RT-PCR analyses revealed that cells in both populations expressed the myocardial marker *TNNT2*. $HCN4^+/SHOX2^+$ cells expressed higher levels of genes associated with the SAN pacemaker, including *HCN4*, *SHOX2*, *ISL1*, and *TBX18* [6,16,17], than $HCN4^+/SHOX2^-$ cells (Fig. 2B). These results suggest that SAN pacemaker-like cells were enriched in the $HCN4^+/SHOX2^+$ cell population.

3.3. Spontaneously beating cells with SAN-like electrophysiological character are contained in $HCN4^+/SHOX2^+$ cell population than $HCN4^+/SHOX2^-$ cell population

To evaluate the electrophysiological properties of $HCN4^+/SHOX2^+$ and $HCN4^+/SHOX2^-$, we measured their APs using the perforated patch-clamp technique, 60 days after CM induction. APs were recorded from spontaneously beating single cells and analyzed for the following: AP interval or beats per minute (BPM); maximum diastolic potential (MDP); peak overshoot potential; AP amplitude (APA); maximal rate of depolarization (dV/dt_max); AP duration (APD) at different levels of repolarization (Supplementary Fig. 5). The APDs were measured at 30%, 40%, 50%, 70%, 80%, and 90% repolarization (denoted as APD30, APD40, APD50, APD70, APD80, and APD90, respectively), as described previously [18] (Supplementary Fig. 5). The "$APD_{30\text{-}40/70\text{-}80}$ ratio" was defined as the difference between APD40 and APD30 (APD40–APD30) divided by the difference between APD70 and APD80 (APD80–APD70).

Both $HCN4^+/SHOX2^+$ and $HCN4^+/SHOX2^-$ cells showed automaticity of the SAN-like, atrial-like, and ventricular-like APs (Fig. 3A). We categorized CMs in each cell population into SAN-like, atrial-like, or ventricular-like CMs according to their $APD_{30\text{-}40/70\text{-}80}$ ratio and dV/dt_max value, as previously reported [5,19]. We first classified $HCN4^+/SHOX2^+$ and $HCN4^+/SHOX2^-$ into ventricular-like CMs ($APD_{30\text{-}40}/APD_{70\text{-}80}$ ratio $\geq$1.5) and non-ventricular-like CMs ($APD_{30\text{-}40/70\text{-}80}$ ratio <1.5). Further, we classified non-ventricular-like CMs into SAN-like CMs (dV/dt_max <10 mV/ms) and atrial-like CMs (dV/dt_max $\geq$10 mV/ms) (Fig. 3B, *left*). Using these criteria, we found that of 37 $HCN4^+/SHOX2^+$, the number (percentage) of SAN-like, atrial-like, and ventricular-like CMs was 26 (70.2%), 3 (8.1%), and 8 (21.6%), respectively. Conversely, of 16 $HCN4^+/SHOX2^-$, 3 $HCN4^+/SHOX2^-$ were SAN-like CMs (18.7%), 4 $HCN4^+/SHOX2^-$ were atrial-like CMs (25.0%), and 9 $HCN4^+/SHOX2^-$ were ventricular-like CMs (56.2%) (Fig. 3B, *right*). In the $HCN4^+/SHOX2^+$, the $APD_{30\text{-}40/70\text{-}80}$ ratios of the SAN-like cells (0.79 ± 0.05) and atrial-like cells (0.79 ± 0.28) were significantly smaller than that of the ventricular-like cells (2.05 ± 0.21). Moreover, the dV/dt_max of the SAN-like cells (4.8 ± 0.4 mV/ms) was significantly smaller than those of the atrial-like cells (14.1 ± 3.6 mV/ms) and ventricular-like cells (9.9 ± 1.1 mV/ms) (Fig. 3C). The APA of the SAN-like cells (69.9 ± 2.4 mV) was significantly smaller than those of the atrial-like cells (93.0 ± 6.6 mV) and ventricular-like cells (87.1 ± 2.8 mV). The BPM of the SAN-like cells (88.7 ± 6.2 b.p.m.) was higher than that of the atrial-like cells (57.9 ± 11.0 b.p.m.) and significantly higher than that of the ventricular-like cells (56.1 ± 13.3 b.p.m.) (Fig. 3D).

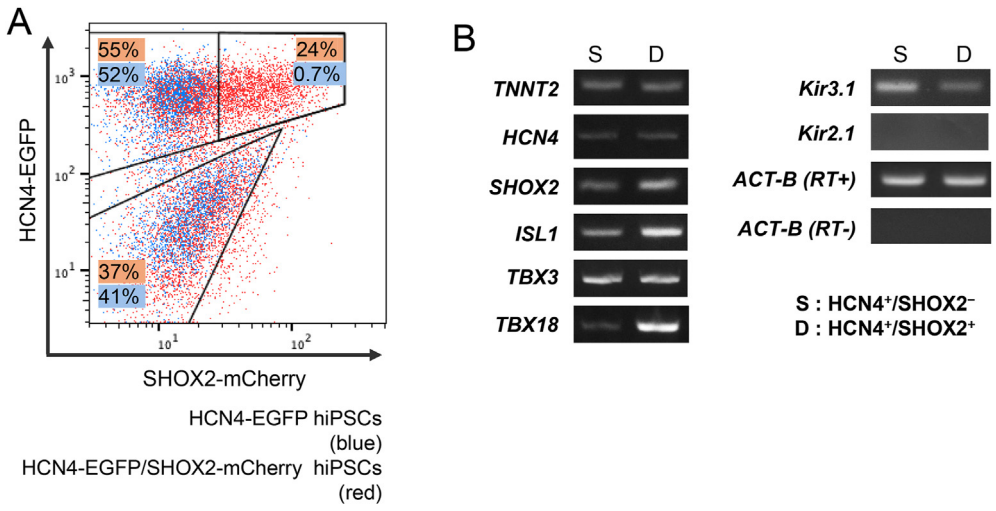

Fig. 2. Isolation and biochemical characterization of HCN4+/SHOX2+ cells and HCN4+/SHOX2-cells. (A) Flow cytometry analysis of cells differentiated from HCN4-EGFP single reporter hiPSCs (blue) and HCN4-EGFP/SHOX2-mCherry dual reporter hiPSCs (red) on day 60. The HCN4+/SHOX2-and HCN4+/SHOX2+ fractions are shown in the upper left and upper right, respectively. HCN4+/SHOX2-and HCN4+/SHOX2+ were isolated by cell sorting (B) mRNA expression levels of SAN marker genes on day 60 of the differentiation in HCN4+/SHOX2-and HCN4+/SHOX2+ as determined by RT-PCR. TNNT2, troponin T2; ACT-B, actin beta.

I_f, a key contributor to spontaneous phase 4 depolarization [20] was detected in the $HCN4^+/SHOX2^+$ that were classified as SAN-like CMs (n = 3), atrial-like CMs (n = 3), and ventricular-like CMs (n = 6) (Fig. 4A) but not in the $HCN4^+/SHOX2^-$. The density of I_f in SAN-like CMs was significantly higher than that in ventricular-like CMs (Fig. 4B). Treatment of the $HCN4^+/SHOX2^+$ SAN-like CMs with the I_f blocker CsCl (2 mM) increased the cycle length of APs by 32.5 ± 4.1% (from 830.1 ± 71.1 ms to 1101.9 ± 125.5 ms, n = 3) (Supplementary Fig. 6A). In addition, we have simulated the effect of I_f block on pacemaker activity of the human SAN cell simulation model [39] and compared thr simulation result with experimental data. The complete block of I_f human SAN cell model prolonged the cycle length of APs by 28.2% (from 813.4 ms to 1042.6 ms) (Supplementary Fig. 6B), which was very close to the experimentally observed effect of the I_f blocker CsCl at 2 mM on human iPSC-derived SAN-type cardiomyocytes.

Carbachol treatment (10 μM) of the SAN-like CMs among the $HCN4^+/SHOX2^+$ slowed their automaticity and decreased their BPM by 18.7 ± 5.88% (60.5 ± 7.9 to 49.6 ± 8.3 b.p.m., n = 3) (Fig. 5A). Subsequent administration of isoproterenol (10 μM) in the presence of carbachol accelerated their automaticity and increased their BPM by 28.4 ± 6.04% (49.6 ± 8.3 to 63.1 ± 9.4 b.p.m., n = 3) (Fig. 5B). Thus, SAN-like CMs in the $HCN4^+/SHOX2^+$ cell population showed autonomic modulation of their automaticity, which is typical of SAN CMs.

4. Discussion

We reported earlier that SHOX2 refined the identification of human SAN-like cells during in vitro cardiac differentiation. HCN4-EGFP/SHOX2-mCherry dual reporter human iPSCs identified subpopulations in HCN4 cell populations and found the presence of $HCN4^+/SHOX2^-$ and $HCN4^+/SHOX2^+$ cells during cardiac differentiation. $HCN4^+/SHOX2^+$ cells appeared to develop from the $HCN4^+/SHOX2^-$ cell population on day 16 and increased their population gradually daily. Comparing $HCN4^+/SHOX2^-$ cells and $HCN4^+/SHOX2^+$ cells, $HCN4^+/SHOX2^+$ cells displayed molecular and electrophysiological properties of human SAN cells than $HCN4^+/SHOX2^-$ cells. Further, 70% of spontaneously beating cells in $HCN4^+/SHOX2^+$ cell populations showed SAN-like electrophysiological characteristics and pharmacological properties.

Previous approaches for the identification of SAN-like cells have used one SAN reporter gene and other markers to detect other cells. An antibody against CD166 expressed in the developing heart tube and sinus venosus has been used as a prospective SAN cell surface marker. However, CD166 expression was transient and might not be useful for the identification of SAN-like cell populations in in vitro cardiac differentiation [7]. In mice, some SAN-specific expression genes were identified from $Tbx3^+$ isolated cell population RNA-Seq data. Nevertheless, each gene was not a SAN-specific expression gene that was classified as neuronal, fibroblast, epicardial, and endocardial genes [21,22]. We used two SAN-specific genes—*HCN4* and *SHOX2*—which are involved in the function and differentiation of SAN, respectively, to collect hiPSC-derived SAN-like cells with spontaneous APs close to those of native cardiac pacemaker cells in vitro.

We classified hiPSC-derived CMs in each cell population as SAN-like, atrial-like, or ventricular-like CMs according to their $APD_{30\text{-}40/70\text{-}80}$ ratio and dV/dt_max value [5,19]. $HCN4^+/SHOX2^+$ SAN-like APs were similar to mammalian and human SAN APs and characterized by slower phase 0 upstroke, earlier phase 3 repolarization (shorter APD), and faster phase 4 depolarization than atrial- and ventricular-like APs [23–27]. Additionally, the SAN-like APs of the $HCN4^+/SHOX2^+$ cells were characterized by depolarized MDP (−53.4 ± 2.4 mV), lower AP peak (16.4 ± 2.5 mV), and smaller APA (66.9 ± 2.4 mV). These results are consistent with previous reports showing hiPSC-derived SAN-like cells with an MDP of approximately −60 mV, a peak below 30 mV, and an APA lower than 80 mV [5,6,19,28,29], whereas AP intervals and APDs differed (Supplementary Table 2). The differences in the AP interval and APD could be caused by differences in the method of hiPSC differentiation and/or in the maturity of SAN-like cells. In the early stages of differentiation, SAN-like cells derived from hiPSCs show slow AP rates and low APAs, reflecting the immaturity of these cells [29]. However, the beating of immature SAN-like cells is faster than that of the human heart at rest with a lack of parasympathetic innervation [6]. In this study, we added *SHOX2* as a marker under the hypothesis that it would clarify the boundary with immature cells expressing HCN4 in the early stages. The proportion of SHOX2-mCherry positive cells increased until day 49, and later showed no change up to day 60. This result with our differentiation induction protocol is interpreted as indicating that the differentiation into a pacemaker was completed around day 49. However, the maturation

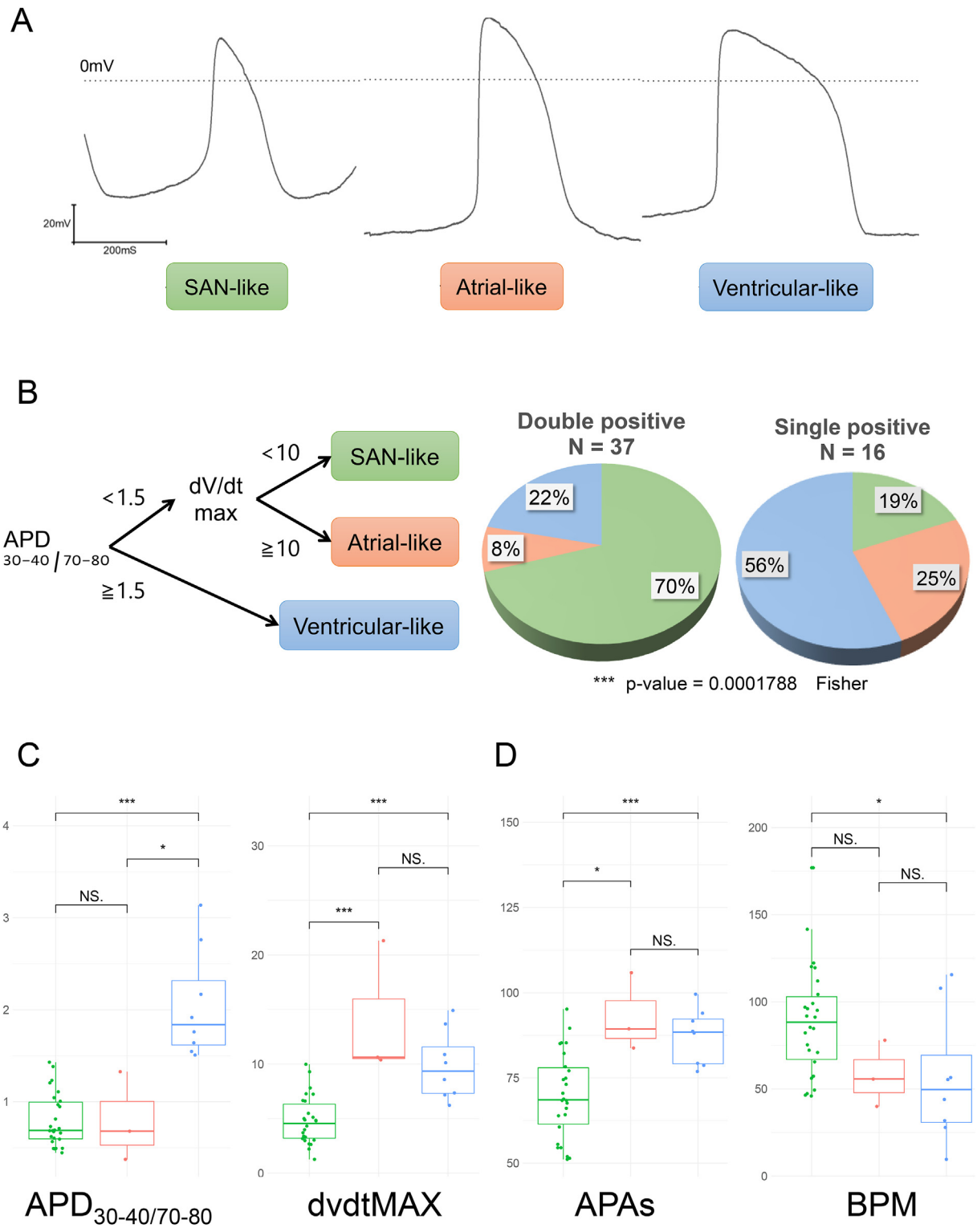

Fig. 3. Electrophysiological characterization of HCN4+/SHOX2+ cells and HCN4+/SHOX2-cells. (A) Representative waveforms of sinoatrial node (SAN)-like, atrial-like, and ventricular-like action potentials (APs) recorded at 37 °C in the HCN4+/SHOX2+ cells (B) Criteria used for the subtype classification of hiPSC-derived CMs by two AP parameters of the APD30-40/70–80 ratio and dV/dt_max (mV/ms). Pie charts show the distribution of SAN-like, atrial-like, and ventricular-like APs of the HCN4+/SHOX2+ double-positive cells (n = 37) and HCN4+/SHOX2-single positive cells (n = 16). Fisher's test: p-value = 0.0001788 (C) Comparisons by boxplots of the APD30-40/70–80 ratio and dV/dt_max (mV/ms) between SAN-like (green), atrial-like (red), and ventricular-like (blue) CMs in the HCN4+/SHOX2+ cell population. Mann–Whitney U test: *p < 0.05, ***p < 0.001 (D) Comparisons by boxplots of the AP amplitude (APA) in mV and beats per minute (BPM) among the three types of CMs in the HCN4+/SHOX2+ population. Mann–Whitney U test: *p < 0.05; ***p < 0.001; NS., not significant.

status of SAN-like cells in the HCN4$^+$/SHOX2$^+$ cell population in our culture system was unclear. Moreover, in other SAN classifications (dV/dt_max <30 mV/ms), every HCN4$^+$/SHOX2$^+$ cell population is categorized as a SAN-like cell AP [6]. Indeed, dV/dt_max values were smaller than those of native atrial and ventricular cells in HCN4$^+$/SHOX2$^+$ atrial-like and ventricular-like cells. On the other hand, since

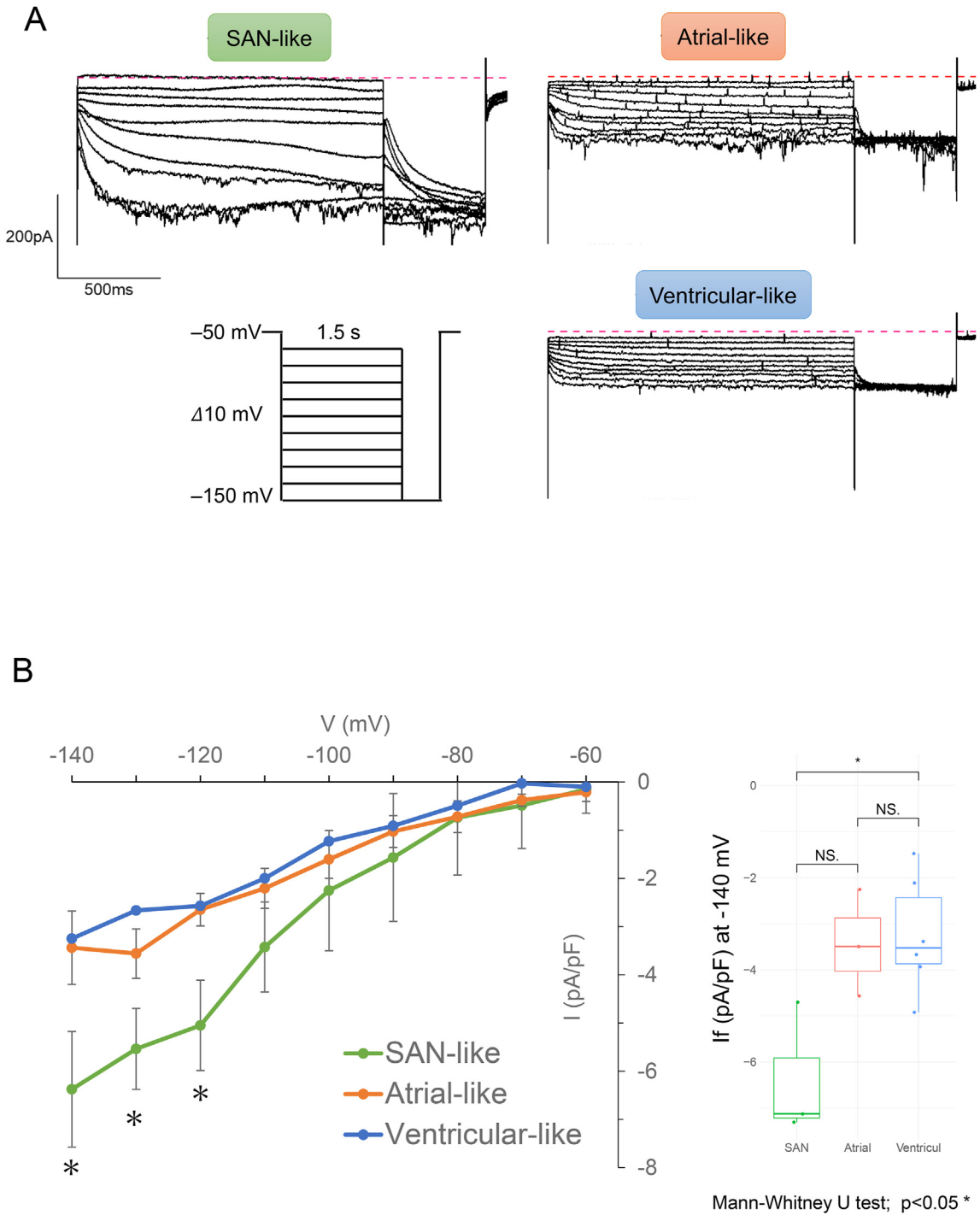

Fig. 4. Characterization of HCN4-mediated hyperpolarization-activated cation channel currents (If) recorded from HCN4+/SHOX2+cells. (A) Representative recordings of If in HCN4+/SHOX2+ cells with SAN-type, atrial-type and ventricular-type APs (inset: voltage protocol). The currents were elicited by 1.5-s hyperpolarizing test pulses with an interpulse interval of 0.5 s (B) Current–voltage relationships determined for If density at the end of test pulses in SAN-like, atrial-like, and ventricular-like HCN4+/SHOX2+ cells. The boxplot on the right panel shows the maximum If densities as determined at the end of a test pulse of −140 mV: SAN-like (green, n = 3), atrial-like (red, n = 3), and ventricular-like (blue, n = 6) HCN4+/SHOX2+cells. Mann–Whitney U test: $p < 0.05$ *.

we have detected atrial (*NR2F2*) and ventricular (*MYL2*) marker gene mRNA expression in $HCN4^+/SHOX2^-$ and $HCN4^+/SHOX2^+$ cell populations on day 60 (Supplementary Fig. 4B), it is possible that both populations contain immature atrial-like and ventricular-like CMs with small dV/dt_max of less than 10 (V/s).

The If current mediated by HCN4 channels was detected in the $HCN4^+/SHOX2^+$ population but not in the $HCN4^+/SHOX2^-$ population. This is a limitation of measuring systems. The success rate of measuring I_f current is low in the case of examining $HCN4^+/SHOX2^+$ cells using our protocol; of 37 $HCN4^+/SHOX2^+$ cells, only 12 cells showed detectable I_f (the success rate = 32%). With the same protocol, we did not identify any measurable I_f currents in $HCN4^+/SHOX2^-$ cells examined (n = 16). Although a small number of $HCN4^+/SHOX2^-$ cells were examined, at least 5 of 16 cells in the

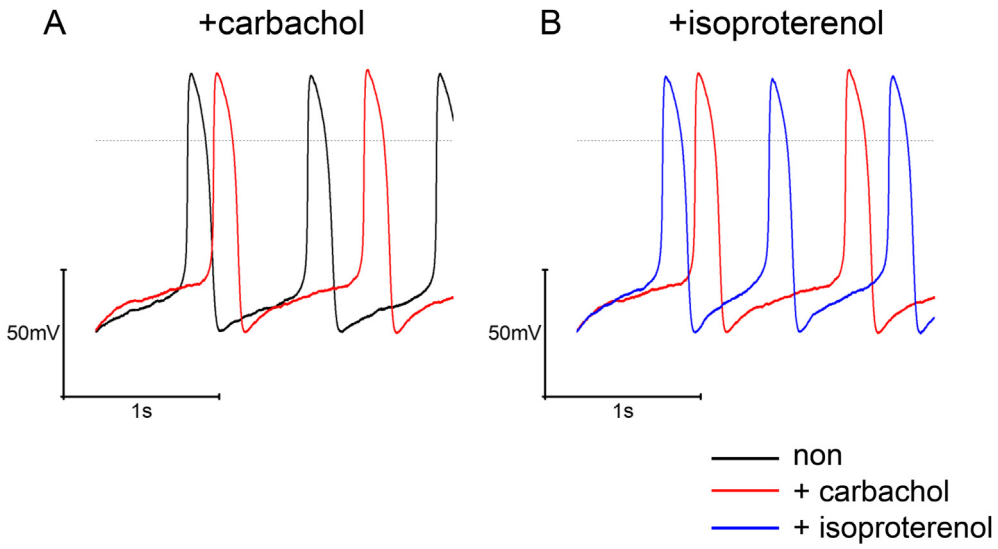

Fig. 5. Effects of carbachol and isoproterenol on SAN-type spontaneous APs of a HCN4+/SHOX2+cells. (A) Spontaneous APs recorded before (black) and after 5 min (red) perfusion with 10 μM carbachol (B) Spontaneous APs recorded after 5 min perfusion with 10 μM carbachol alone (red) and 5 min perfusion with 10 μM isoproterenol in the presence of 10 μ carbachol (blue).

calculation would provide I_f current in the case that they have functional I_f channels. Therefore, it seems that functional I_f channels are not expressed in SHOX2-negative (HCN4 single positive) cells; $HCN4^+/SHOX2^-$ cells could not express functional I_f channels on the sarcolemmal membrane while expressing HCN4 proteins in the cytoplasm. We consider that the expression of genes (proteins) transcriptionally regulated by SHOX2 may be required directly or indirectly for the expression of functional I_f channels on the sarcolemmal membrane. The mechanisms of regulation of ion channel expression by transcription factors are not well understood and are a subject for future research.

HCN4 is also expressed in the mouse CCS, including the atrioventricular node, His bundles, and Purkinje fibers, but not in atrial or ventricular-type CMs [22]. Although APs of human CCS cells other than Purkinje fiber cells have not yet been recorded [30], CCS cells in other mammals have been shown to be involved in several AP types, including those similar to atrial and ventricular APs [31,32]. Recently, human Purkinje fiber APs have been reported to have a faster depolarization phase, a more negative plateau, and longer APD than ventricular APs [33]. $HCN4^+/SHOX2^+$ cells with atrial-like and ventricular-like APs may be categorized as CCS cells rather than SAN cells.

Our results showed that approximately 70% of the $HCN4^+/SHOX2^+$ cell population exhibited electrophysiological characteristics of SAN-like CMs. However, the remaining 30% of cells were not SAN-like. This is a limitation in identifying human SAN-like cells using reporter systems. To improve the identification of human SAN-like cells, it is necessary to have a detailed understanding of human SAN cells and optimize the method for inducing differentiation into human SAN cells. In recent years, various cardiac cell differentiation methods have been reported for each CM subtype [34]. In addition to the regulation of WNT signaling, either the combined modulation of BMP, fibroblast growth factor (FGF), and retinoic acid (RA) signaling pathways or the inhibition of NODAL signaling promotes the differentiation of hiPSCs into SAN-like cells [35–37]. Here, the GiWi method—a modified version of Yamauchi's cardiac cell differentiation induction method (the Gi method)—led to a higher prevalence of HCN4-EGFP-positive cells, which comprised more than seven times of the Gi method [14,15] (Fig. 1C, Supplementary Fig. 2B). The difference between the GiWi and Gi method is that the Wnt inhibitor IWP2 is administered on day 4 in the GiWi method but not in the Gi method, our results suggesting that inhibition of WNT signaling causes a change in the induction of cell fate. In the Gi method, HCN4-positive cells, more than 50% in the early stage or on day 14, decreased at a relatively rapid rate during cardiac differentiation, suggesting that HCN4-negative cells in the late stage are FHF-derived cells such as mature left ventricular and atrial CMs that do not express HCN4 in the late stage [42]. Although the details are unclear from this study, it is shown that the GiWi method is more suitable than the Gi method for inducing cells expressing HCN4 in the later stages. Further analysis is required to determine the optimal culture conditions for SAN-like cell induction.

In a previous study of hiPSC-derived SAN-like cells, two SAN types showed different electrophysiological characteristics: central SAN and peripheral SAN [29]. In this study, each SAN type was observed and classified into the same SAN-like APs. Various AP shapes and gene expressions have not been matched to SAN at the single-cell level, and it is unclear which genes correspond to AP configurations. If the AP shapes and gene expression can be verified in single cells, identifying and analyzing the characteristics of native SAN cells will become a possibility.

In summary, we enriched SAN-like cells by developing HCN4-EGFP/SHOX2-mCherry dual reporter hiPSCs, which was confirmed by visualizing HCN4 and SHOX2 gene expression with fluorescent proteins. The enrichment of human SAN-like cells derived from hiPSCs will help test the cardiotoxic and chronotropic effects of novel drug candidates. To date, the cardiotoxic effects of novel drug candidates have been tested in mammalian cells expressing hERG channels [38]. However, human CMs express several types of ion channels, including hERG channels. Using human CMs derived from hiPSCs is an appropriate method to characterize human cardiac ion channels in detail. Many companies have recently sold hiPSC-derived CMs. However, these populations include various CM subtypes, although they mostly comprise ventricular-like CMs [5,28]. Thus, the HCN4-EGFP/SHOX2-mCherry dual reporter hiPSCs developed in this study provide a useful system for purifying SAN-like CMs as in vitro models of human SAN cells.

5. Conclusions

We established a HCN4-EGFP/SHOX2-mCherry dual reporter hiPSC system. Notably, 70% of HCN4/SHOX2 double-positive cells isolated from differentiated hiPSC-derived CM populations showed biochemical and electrophysiological properties of SAN cells. This hiPSC system enabled the enrichment of SAN-like cells derived from a mixed population of differentiating cardiac cells. Enrichment of human SAN-like cells is useful for testing the cardiotoxic and chronotropic effects of novel drug candidates, as well as for regenerative medicine, such as the development of hiPSC-derived biological pacemakers.

Authors' contributions

Takayuki Wakimizu: Planning and performing the experiments, including the establishment of Shox2-mCherry cell line, data analysis and interpretation, manuscript writing.

Kumi Morikawa: Establishment of experimental system, support for conceptualization of this study

Kenta Fukumura: Establishment of HCN4-EGFP cell line

Tetsuo Yuki: Acquisition analysis of data

Takashi Adachi: Acquisition analysis of data

Yasutaka Kurata: Computational simulation, data analysis, and interpretation

Junichiro Miake: Data analysis and interpretation, manuscript writing

Ichiro Hisatome: Data analysis and interpretation, supervision of the study

Motokazu Tsuneto: Planning and performing the experiments, supervising the experiments, manuscript writing

Yasuaki Shirayoshi: Conceptualization and supervision of the study

Ethics approval and consent to participate

Not applicable.

Consent for publication

Not applicable.

Availability of data and materials

The datasets used and/or analyzed during this study are available from the corresponding author upon reasonable request.

Funding

This work was supported by JSPS KAKENHI grant JP20K22514 to K.M. and grants JP17K08539/JP20K12623 to Y.S. and the Cooperative Research Program (Joint Usage/Research Center program) of the Institute for Frontier Life and Medical Sciences, Kyoto University to Y.S.

Declarations of interest

None.

Acknowledgments

We thank Y. Nakayama at the Organization for Research Initiative and Promotion, Tottori University, for cell sorting and S. Itou for the initial work on this project. This work was supported by JSPS KAKENHI grants JP15K21170/JP25893134/JP12J00001 to K.M. and grants JP17K08539/JP20K12623 to Y.S. and the Cooperative Research Program (Joint Usage/Research Center program) of the Institute for Frontier Life and Medical Sciences, Kyoto University, to Y.S..

Appendix A. Supplementary data

Supplementary data to this article can be found online at https://doi.org/10.1016/j.reth.2022.07.012.

References

[1] Servatius H, Porro A, Pless SA, Schaller A, Asatryan B, Tanner H, et al. Phenotypic spectrum of HCN4 mutations: a clinical case. Circ Genom Precis Med 2018;11:e002033. https://doi.org/10.1161/CIRCGEN.117.002033.

[2] Takahashi K, Tanabe K, Ohnuki M, Narita M, Ichisaka T, Tomoda K, et al. Induction of pluripotent stem cells from adult human fibroblasts by defined factors. Cell 2007;131:861–72. https://doi.org/10.1016/j.cell.2007.11.019.

[3] Loh KMM, Chen A, Koh PWW, Deng TZZ, Sinha R, Tsai JMM, et al. Mapping the pairwise choices leading from pluripotency to human bone, heart, and other mesoderm cell types. Cell 2016;166:451–67. https://doi.org/10.1016/j.cell.2016.06.011.

[4] Mummery CL, Zhang J, Ng E, Elliott DA, Elefanty AG, Kamp TJ. Differentiation of human ES and iPS cells to cardiomyocytes: a methods overview. Circ Res 2012;111:344–58. https://doi.org/10.1161/CIRCRESAHA.110.227512.Differentiation.

[5] Ma J, Guo L, Fiene SJ, Anson BD, Thomson JA, Kamp TJ, et al. High purity human-induced pluripotent stem cell-derived cardiomyocytes: electrophysiological properties of action potentials and ionic currents. Am J Physiol Heart Circ Physiol 2011;301:H2006–17. https://doi.org/10.1152/ajpheart.00694.2011.

[6] Protze SI, Liu J, Nussinovitch U, Ohana L, Backx PH, Gepstein L, et al. Sinoatrial node cardiomyocytes derived from human pluripotent cells function as a biological pacemaker. Nat Biotechnol 2017;35:56–68. https://doi.org/10.1038/nbt.3745.

[7] Scavone A, Capilupo D, Mazzocchi N, Crespi A, Zoia S, Campostrini G, et al. Embryonic stem cell-derived CD166+ precursors develop into fully functional sinoatrial-like cells. Circ Res 2013;113:389–98. https://doi.org/10.1161/CIRCRESAHA.113.301283.

[8] Fedorov VV, Glukhov AV, Chang R. Conduction barriers and pathways of the sinoatrial pacemaker complex: their role in normal rhythm and atrial arrhythmias. Am J Physiol Heart Circ Physiol 2012;302:H1773–83. https://doi.org/10.1152/ajpheart.00892.2011.

[9] Kojima A, Matsuura H. Ionic mechanisms of the action of anaesthetics on sinoatrial node automaticity. Eur J Pharmacol 2017;814:63–72. https://doi.org/10.1016/j.ejphar.2017.08.006.

[10] Morikawa K, Bahrudin U, Miake J, Igawa O, Kurata Y, Nakayama Y, et al. Identification, isolation and characterization of HCN4-positive pacemaking cells derived from murine embryonic stem cells during cardiac differentiation. Pacing Clin Electrophysiol 2010;33:290–303. https://doi.org/10.1111/j.1540-8159.2009.02614.x.

[11] Liang X, Wang G, Lin L, Lowe J, Zhang Q, Bu L, et al. HCN4 dynamically marks the first heart field and conduction system precursors. Circ Res 2013;113:399–407. https://doi.org/10.1161/CIRCRESAHA.113.301588.

[12] Liu H, Espinoza-Lewis RA, Chen C, Hu X, Zhang Y, Chen YP. The role of Shox2 in SAN development and function. Pediatr Cardiol 2012;33:882–9. https://doi.org/10.1007/s00246-012-0179-x.

[13] Okita K, Matsumura Y, Sato Y, Okada A, Morizane A, Okamoto S, et al. A more efficient method to generate integration-free human iPS cells. Nat Methods 2011;8:409–12. https://doi.org/10.1038/nmeth.1591.

[14] Yamauchi K, Sumi T, Minami I, Otsuji TG, Kawase E, Nakatsuji N, et al. Cardiomyocytes develop from anterior primitive streak cells induced by β-catenin activation and the blockage of BMP signaling in hESCs. Gene Cell 2010;15:1216–27. https://doi.org/10.1111/j.1365-2443.2010.01455.x.

[15] Lian X, Zhang J, Azarin SM, Zhu K, Hazeltine LB, Bao X, et al. Directed cardiomyocyte differentiation from human pluripotent stem cells by modulating Wnt/β-catenin signaling under fully defined conditions. Nat Protoc 2013;8:162–75. https://doi.org/10.1038/nprot.2012.150.

[16] Sizarov A, Devalla HD, Anderson RH, Passier R, Christoffels VM, Moorman AFM. Molecular analysis of patterning of conduction tissues in the developing human heart. Circ Arrhythm Electrophysiol 2011;4:532–42. https://doi.org/10.1161/CIRCEP.111.963421.

[17] Christoffels VM, Smits GJ, Kispert A, Moorman AFM. Development of the pacemaker tissues of the heart. Circ Res 2010;106:240–54. https://doi.org/10.1161/CIRCRESAHA.109.205419.

[18] Logantha SJRJ, Kharche SR, Zhang Y, Atkinson AJ, Hao G, Boyett MR, et al. Sinus node-like pacemaker mechanisms regulate ectopic pacemaker activity in the adult rat atrioventricular ring. Sci Rep 2019;9:1–16. https://doi.org/10.1038/s41598-019-48276-0.

[19] Fukushima H, Yoshioka M, Kawatou M, López-Dávila V, Takeda M, Kanda Y, et al. Specific induction and long-term maintenance of high purity ventricular cardiomyocytes from human induced pluripotent stem cells. PLoS One 2020;15:e0241287. https://doi.org/10.1371/journal.pone.0241287.
[20] Lakatta EG, DiFrancesco D. What keeps us ticking: a funny current, a calcium clock, or both? J Mol Cell Cardiol 2009;47:157–70. https://doi.org/10.1016/j.yjmcc.2009.03.022.
[21] van Eif VWW, Stefanovic S, van Duijvenboden K, Bakker M, Wakker V, de Gier-de Vries C, et al. Transcriptome analysis of mouse and human sinoatrial node cells reveals a conserved genetic program. Development 2019;146. https://doi.org/10.1242/dev.173161.
[22] Goodyer WR, Beyersdorf BM, Paik DT, Tian L, Li G, Buikema JW, et al. Transcriptomic profiling of the developing cardiac conduction system at single-cell resolution. Circ Res 2019;125:379–97. https://doi.org/10.1161/CIRCRESAHA.118.314578.
[23] Yanagihara K, Noma A, Irisawa H. Reconstruction of sino-atrial node pacemaker potential based on the voltage clamp experiments. Jpn J Physiol 1980;30:841–57. https://doi.org/10.2170/jjphysiol.30.841.
[24] Nakayama T, Kurachi Y, Noma A, Irisawa H. Action potential and membrane currents of single pacemaker cells of the rabbit heart. Pflugers Arch 1984;402:248–57. https://doi.org/10.1007/BF00585507.
[25] Verkerk AO, Wilders R, Van Borren MMGJ, Tan HL. Is sodium current present in human sinoatrial node cells? Int J Biol Sci 2009;5:201–4. https://doi.org/10.7150/ijbs.5.201.
[26] Verkerk AO, Wilders R, Van Borren MMGJ, Peters RJG, Broekhuis E, Lam K, et al. Pacemaker current (If) in the human sinoatrial node. Eur Heart J 2007;28:2472–8. https://doi.org/10.1093/eurheartj/ehm339.
[27] Drouin E. Electrophysiologic properties of the adult human sinus node. J Cardiovasc Electrophysiol 1997;8:254–8. https://doi.org/10.1111/j.1540-8167.1997.tb00788.x.
[28] Yonemizu S, Masuda K, Kurata Y, Notsu T, Higashi Y, Fukumura K, et al. Inhibitory effects of class I antiarrhythmic agents on Na+ and Ca2+ currents of human iPS cell-derived cardiomyocytes. Regen Ther 2019;10:104–11. https://doi.org/10.1016/j.reth.2018.12.002.
[29] Schweizer PA, Darche FF, Ullrich ND, Geschwill P, Greber B, Rivinius R, et al. Subtype-specific differentiation of cardiac pacemaker cell clusters from human induced pluripotent stem cells. Stem Cell Res Ther 2017;8:229. https://doi.org/10.1186/s13287-017-0681-4.
[30] Nagy N, Szél T, Jost N, Tóth A, Gy Papp JG, Varró A. Novel experimental results in human cardiac electrophysiology: measurement of the Purkinje fibre action potential from the undiseased human heart. Can J Physiol Pharmacol 2015;93:803–10. https://doi.org/10.1139/cjpp-2014-0532.
[31] Zhang H, Holden AV, Kodama I, Honjo H, Lei M, Varghese T, et al. Mathematical models of action potentials in the periphery and center of the rabbit sinoatrial node. Am J Physiol Heart Circ Physiol 2000;279:H397–421. https://doi.org/10.1152/ajpheart.2000.279.1.H397.
[32] Verkerk AO, Veldkamp MW, Abbate F, Antoons G, Bouman LN, Ravesloot JH, et al. Two types of action potential configuration in single cardiac Purkinje cells of sheep. Am J Physiol - Hear Circ Physiol 1999;277:H1299–310. https://doi.org/10.1152/ajpheart.1999.277.4.H1299.
[33] Trovato C, Passini E, Nagy N, Varró A, Abi-Gerges N, Severi S, et al. Human Purkinje in silico model enables mechanistic investigations into automaticity and pro-arrhythmic abnormalities. J Mol Cell Cardiol 2020;142:24–38. https://doi.org/10.1016/j.yjmcc.2020.04.001.
[34] Protze SI, Lee JH, Keller GM. Human pluripotent stem cell-derived cardiovascular cells: from developmental biology to therapeutic applications. Cell Stem Cell 2019;25:311–27. https://doi.org/10.1016/j.stem.2019.07.010.
[35] Liu F, Fang Y, Hou X, Yan Y, Xiao H, Zuo D, et al. Enrichment differentiation of human induced pluripotent stem cells into sinoatrial node-like cells by combined modulation of BMP, FGF, and RA signaling pathways. Stem Cell Res Ther 2020;11:284. https://doi.org/10.1186/s13287-020-01794-5.
[36] Ren J, Han P, Ma X, Farah EN, Bloomekatz J, Zeng XI, et al. Canonical Wnt5b signaling directs outlying Nkx2.5+ mesoderm into pacemaker cardiomyocytes. Dev Cell 2019;50:729–43. https://doi.org/10.1016/j.devcel.2019.07.014. e5.
[37] Yechikov S, Kao HKJ, Chang CW, Pretto D, Zhang XD, Sun YH, et al. NODAL inhibition promotes differentiation of pacemaker-like cardiomyocytes from human induced pluripotent stem cells. Stem Cell Res 2020;49:102043. https://doi.org/10.1016/j.scr.2020.102043.
[38] Wible BA, Hawryluk P, Ficker E, Kuryshev YA, Kirsch G, Brown AM. HERG-Lite®: a novel comprehensive high-throughput screen for drug-induced hERG risk. J Pharmacol Toxicol Methods 2005;52:136–45. https://doi.org/10.1016/j.vascn.2005.03.008.
[39] Fabbri A, Fantini M, Wilders R, Severi S. Computational analysis of the human sinus node action potential: model development and effects of mutations. J Physiol 2017;595:2365–96. https://doi.org/10.1113/JP273259.
[40] Kurata Y, Hisatome I, Imanishi S, Shibamoto T. Dynamical description of sinoatrial node pacemaking: improved mathematical model for primary pacemaker cell. Am J Physiol Heart Circ Physiol 2002;283:H2074–101. https://doi.org/10.1152/ajpheart.00900.2001.
[41] Kurata Y, Matsuda H, Hisatome I, Shibamoto T. Roles of hyperpolarization-activated current i_f in sinoatrial node pacemaking: insights from bifurcation analysis of mathematical models. Am J Physiol Heart Circ Physiol 2010;298:H1748–60. https://doi.org/10.1152/ajpheart.00729.2009.
[42] Später D, Abramczuk MK, Buac K, Zangi L, Stachel MW, Clarke J, et al. A HCN4+ cardiomyogenic progenitor derived from the first heart field and human pluripotent stem cells. Nat Cell Biol 2013;15:1098–106. https://doi.org/10.1038/ncb2824.